

Adsorption Dynamics of a Phospholipase A₂ onto a Mercury Electrode Surface

Shaowei Chen and Héctor D. Abruña*

Department of Chemistry, Baker Laboratory, Cornell University, Ithaca, New York 14853-1301

Received: June 16, 1995; In Final Form: September 9, 1995[⊗]

Rapid cyclic voltammetry has been employed to investigate the electrochemical behavior of porcine pancreatic phospholipase A₂ (PLA₂) adsorbed onto a hanging mercury drop electrode surface. The electrochemical response of PLA₂ exhibits a pair of voltammetric peaks which are ascribed to the reduction/oxidation of cystine/cysteine residues within the enzyme strongly adsorbed on mercury surfaces over the pH range of 0.77–8.50. Based on theoretical fits to the data, the adsorption process, under all experimental conditions, is found to be kinetically controlled. In addition, the adsorption appears to be consistent with a Frumkin adsorption isotherm with a small repulsive interaction. Both pH and temperature have a dramatic effect on the adsorption behavior in terms of the adsorption rate, equilibrium coverage, and molecular conformation.

Introduction

Phospholipases A₂ (PLA₂, EC 3.1.1.4) are a family of ubiquitous, small, water-soluble lipolytic enzymes, which can be found both inside and outside cells. Many of these enzymes are highly homologous in amino acid sequences despite a wide variety of sources. As phospholipases A₂ specifically catalyze the hydrolysis of the 2-acyl ester linkage of 3-*sn*-glycerophospholipids, releasing the corresponding lysophospholipids and fatty acids, there have been extensive studies geared at the understanding of the protein–lipid interaction involved in this hydrolysis process, of the biological significance of the hydrolytic products which play an important role in the metabolism cycles, and of the mechanism of transmembrane signal transfer by the second messengers played by the released fatty acids (for reviews, see refs 1 and 2). Although phospholipases A₂ can be found both within and without the cell, the extracellular enzymes have been more widely studied and are better understood, partly because the studies of the intracellular enzymes have been complicated by the variation of the subcellular site of their intracellular location as well as by the interference of phospholipases A₁ (which hydrolyze the 1-acyl ester linkage), as both of them coexist in many cells. Extracellular phospholipases A₂ are abundant in pancreatic tissue and juice and in the venom of snakes and arthropods. Their 3-dimensional structures, active site structures, and interface recognition site (IRS) structures have been characterized by X-ray crystallographic studies.^{3–5} Due to their high affinity and activity to aggregated assemblies of phospholipids (e.g., monolayers, bilayers, micelles, vesicles, and membranes), the so-called “interfacial activation”, phospholipases A₂ have been used widely to study catalytic hydrolysis effects on these model biological membranes, providing much information about the actual biological processes.^{6–13} Since phospholipases, as well as phospholipids, are generally charged, their interaction depends strongly on their electric properties.¹⁴ Thus, electrochemistry can be very effective in providing new insights on their properties, due to the high mechanical stability and strong resistance of model biological membranes to electrode potential.

Although a number of electrochemical studies of phospholipid adlayers have been reported,¹⁵ such is not the case for phospholipases. In order to better understand this biologically important system, we have carried out a cyclic voltammetric study of porcine pancreatic phospholipase A₂ (PLA₂), in terms

of the effects of sweep rate, concentration, pH, and temperature, from which kinetic and thermodynamic parameters related to the adsorption process can be extracted. These studies can then be used as a starting point for a comprehensive study of the lipid–protein interaction by interfacial techniques.

Experimental Section

1. Materials. Porcine pancreatic phospholipase A₂ (PLA₂) (from Sigma, originally suspended in 3.2 M (NH₄)₂SO₄ solution, pH 5.4, with a concentration of 6.3 mg/mL) was used as received. Electrolyte solutions were prepared with ultrapure salts (Aldrich) which were at least of 99.99+% purity. These were dissolved (0.20 M) in water which was purified with a Millipore Milli-Q system and buffered with high-purity acetate or phosphate salts or hydrochloric acid (all from Aldrich) depending on the desired pH.

2. Equipment. Electrochemical experiments were carried out with an EG&G PARC 173 potentiostat and 175 a universal programmer. Data were collected on a Nicolet 4094 digital oscilloscope and transferred to a personal computer for analysis.

In all experiments, a Kemula type hanging mercury drop electrode (HMDE, from Metrohm) was used as the working electrode with a drop area of 1.82 mm². Electronic grade mercury (99.9998% from Johnson Matthey) was employed. A saturated Ag/AgCl electrode was used as a reference electrode, and a large area platinum coil was used as a counter electrode. A two-compartment cell with a medium porosity glass frit was employed in all experiments. The cell had standard taper joints for all electrodes and for degassing.

3. Experimental Procedure. For PLA₂ adsorption studies, 1.0 μL of PLA₂ solution was injected with a microliter syringe into a pipetted volume of working electrolyte solution depending on the desired PLA₂ concentration, which had been degassed for at least an hour using high-purity nitrogen that was additionally passed through oxygen and hydrocarbon traps from MG Industries. In temperature dependence studies, the electrochemical cell (with degassed electrolyte and PLA₂) was placed in an Allied water circulation pool (Fisher Scientific Model 800). At each temperature, at least 40 min was allowed so as to achieve temperature equilibrium before the electrochemical measurements were initiated.

In all experiments, the electrode was under potential control during the entire adsorption process with the applied potential being varied with solution pH: 0.0 V at pH = 0.77 and 2.43,

[⊗] Abstract published in *Advance ACS Abstracts*, November 1, 1995.

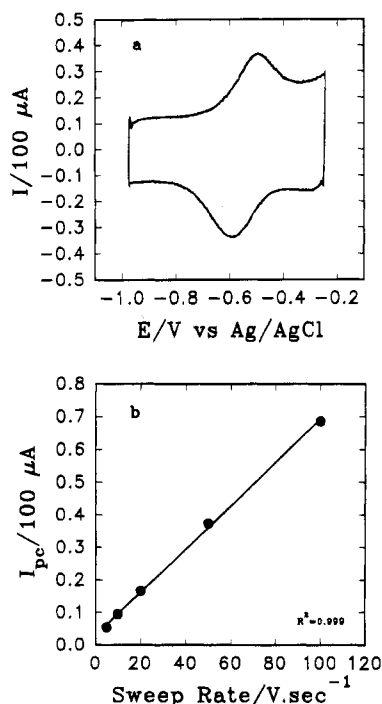


Figure 1. (a) Cyclic voltammogram of PLA₂ adsorbed onto a mercury electrode in 0.20 M KCl buffered with 0.01 M K₂HPO₄–KH₂PO₄ (pH 6.7). Sweep rate is 50 V/s, electrode surface area is 1.82 mm², and PLA₂ concentration is 0.030 μM. (b) Cathodic peak current vs sweep rate.

–0.20 V at pH = 4.64, and –0.25 V at pH = 6.70 and 8.50 (all vs Ag/AgCl). It should also be mentioned that the system was under a nitrogen flow throughout the entire procedure and at room temperature (21–22 °C) unless otherwise specified.

4. Data Analysis. To determine the surface coverage (Γ) of PLA₂, the cathodic peak due to adsorbed PLA₂ was integrated by using PEAKFIT. Since all experiments were carried out at high sweep rate (at least 10 V/s) and the solution concentration of PLA₂ was low (in the micromolar regime), the contribution from dissolved PLA₂ to the total current was deemed negligible compared to the current arising from the adsorbed PLA₂. Thus, the charge (Q) under the wave due to the adsorbed PLA₂ could be employed in the determination of the surface coverage (Γ) using

$$\Gamma = Q/nAF \quad (1)$$

where A is the electrode surface area, F is Faraday's constant, and n is the number of electrons involved in the redox reaction which in the present case equals 2. Details will be discussed further below.

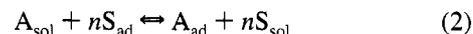
Results and Discussion

1. Characterization of the Electrochemical Responses of PLA₂. We begin with a description of the cyclic voltammetric response of PLA₂ adsorbed onto a mercury surface. As can be seen in Figure 1a, there are two well-defined peaks in the potential range of 0.0 to –1.0 V (vs Ag/AgCl). Their peak currents are proportional to the sweep rate (Figure 1b presents a plot of the cathodic peak current, I_{pc} , vs sweep rate, ν), indicating that they are due to an electrochemical reaction involving adsorbed species. As to the origin of these peaks, it is most likely that they are due to the reduction/oxidation of the disulfide bonds of the cystine residues in the enzyme adsorbed on the mercury surface. Several groups have studied the electrochemical behavior of free cysteine/cystine on mercury

electrode surfaces using cyclic voltammetric and polarographic techniques (ref 16; for reviews, see ref 17). In contrast to the free cystine case where an adsorption wave and a diffusion-controlled wave were observed, the PLA₂ only showed a single adsorption voltammetric wave. This could be due to the strong adsorption of PLA₂ and, consequently, its bulky physical size blocking any contribution from the diffusion of the enzyme. In addition, the solution concentration of PLA₂ was so low (nanomolar to micromolar) that its contribution to the overall current would be negligible. Although there are a total of seven disulfide bonds within a monomeric porcine pancreatic PLA₂ molecule, which rigidly maintain the molecular conformation,¹⁸ it would be energetically unfavorable to have an adsorption conformation of the enzyme with more than one disulfide group attached to the mercury surface. Thus, it is most likely that there is only one disulfide group adsorbed onto the mercury surface. However, it is quite difficult to determine by electrochemical means which specific disulfide group is adsorbed onto the mercury surface. Based on X-ray studies of the 3-dimensional structure of PLA₂ and considering the charge distribution within the PLA₂ molecule, some of the disulfide bonds would appear to be more likely to be adsorbed because of their relative position. An especially likely candidate would be Cys61–Cys91, and we believe that this is the disulfide bond responsible for the observed electrochemical response. However, we must emphasize that at the present time we have no direct evidence in support of this.

For a better understanding of the adsorption process, it is necessary to have a knowledge not only of the thermodynamics but also of the kinetic behavior. In the following we present an experimental study of the thermodynamics as well as the kinetics of the adsorption of PLA₂ onto a hanging mercury drop electrode surface, including the dependencies on PLA₂ concentration, solution pH, and temperature.

2. Thermodynamics of Adsorption. For an adsorption process on an electrode surface to occur, surface sites must be available, where the solution species (A_{sol}) displace the pre-adsorbed species (S_{ad}) which could be solvent molecules. Thus, the adsorption equilibrium can be expressed as



A variety of adsorption isotherms have been proposed to account for the relationship between the amount of adsorbed species (A_{ad}) on the electrode surface, Γ (surface coverage), and its corresponding activity in bulk solution, a^* ,^{19,20} with one of the main differences being the type of adsorbate–adsorbate interactions included. Among these, the Langmuir adsorption isotherm is the simplest where the only adsorbate–adsorbate interaction is due to physical size. However, no other interaction is assumed. Implicit in this is that the free energy of adsorption (ΔG_{ad}) is independent of coverage. The Langmuir adsorption isotherm can be expressed as

$$\beta a^* = \Gamma/(\Gamma_s - \Gamma) \quad (3a)$$

$$\beta a^* = \theta/(1 - \theta) \quad (3b)$$

where $\beta = \exp(-\Delta G_{ad}/RT)$ is the adsorption coefficient, Γ_s is the saturation surface coverage, and $\theta = \Gamma/\Gamma_s$ is the fractional coverage.

If interactions, attractive or repulsive, between the adsorbed species are present, then an exponential term is added to the Langmuir isotherm to take into account such effects. One of the simpler isotherms which includes adsorbate–adsorbate interactions is the Frumkin isotherm, which is given by

$$\beta a^* = \frac{\Gamma}{\Gamma_s - \Gamma} \exp\left(\frac{2g\Gamma}{RT}\right) \quad (4a)$$

where the parameter g describes the way in which the adsorption free energy varies with surface coverage. If g is positive, the interactions between adsorbed species are attractive, and if g is negative, the interactions are repulsive. It is also clear from eq 4a that as $g \rightarrow 0$, the Frumkin isotherm approaches the Langmuir isotherm. Equation 4a can also be expressed as

$$\beta a^* = \frac{\theta}{1 - \theta} \exp(g'\theta) \quad (4b)$$

with $g' = 2g\Gamma_s/RT$.

It should be noted that although the above isotherms require knowledge of the adsorbate activity in the bulk solution (a^*), in our system the adsorbate concentrations are so low that the activity coefficient (γ) can be, to a good approximation, assumed to be unity; thus, the corresponding bulk concentrations (C^*) can be used in place of a^* .

Figure 2 shows adsorption data for PLA₂ onto a mercury surface as well as fits to eqs 3a and 4a, from which it can be seen that although both fits are quite good, a slightly better fit to the Frumkin isotherm is obtained. The fitting parameters are shown in Table 1, where it is apparent that there are only small differences among them. For the Frumkin isotherm, the value of g' (-0.7 ± 0.3) was found to be relatively small, indicating that adsorbate–adsorbate interactions are not very significant. In addition, its negative sign indicates that the nature of the interactions is repulsive. Since in this case the solution pH (6.7) was below the pI of PLA₂ (7.4),¹⁴ the PLA₂ molecules are positively charged, which could be responsible, at least in part, for the repulsive interactions between them. The adsorption free energy (ΔG_{ad}) obtained from both fits is virtually identical, -44 kJ/mol, and its magnitude is consistent with a chemisorptive bond. Also, the saturation coverages (Γ_s) are also very close to each other: 2.7×10^{-11} mol/cm² for the Langmuir and 2.6×10^{-11} mol/cm² for the Frumkin isotherms, which correspond to an area per molecule of 606 and 639 Å², respectively, assuming a close packed 2-dimensional structure. Considering the molecular shape of PLA₂ which is approximately ellipsoidal,²¹ the molecular area estimated from the saturation coverage suggests that the adsorbed site is likely located on one of the elongated ends of the molecule. Partly on the basis of this, we believe that the Cys61-Cys91 is likely the site of adsorption, as mentioned earlier. It can be seen in Figure 2 that although the Langmuir isotherm does not take into account adsorbate–adsorbate interactions, it is still in qualitative agreement with the experimental data. We have previously observed a similar situation in a study of the thermodynamics of adsorption of redox-active self-assembling monolayers of transition metal complexes, where fits to a Frumkin isotherm were slightly better than to a Langmuir isotherm with also a small repulsive interaction parameter ($g' = -0.2$).²²

It can be concluded that although the PLA₂ molecules are charged, their repulsive interactions are not very significant, probably due to the large physical size of the molecules. Thus, the Langmuir isotherm describes the experimental data qualitatively well, despite the fact that it ignores the adsorbate–adsorbate interaction. Because of the small magnitude of g' and the simplicity of the Langmuir isotherm, we have opted to use the Langmuir isotherm to describe the experimental data in further discussion.

3. Kinetics of Adsorption. We have previously discussed the adsorption kinetics of redox-active self-assembling mono-

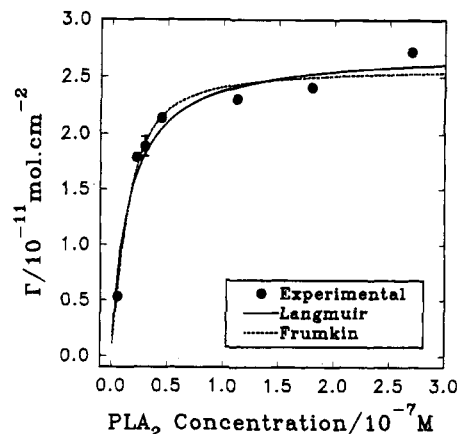


Figure 2. Adsorption isotherms of PLA₂ in 0.20 M KCl at pH = 6.70 and at room temperature.

TABLE 1: Fitting Parameters for the Langmuir and Frumkin Isotherms

fitting parameters	Langmuir	Frumkin
g'	0	-0.7 ± 0.3
β	$(6.6 \pm 1.5) \times 10^7$	$(4.5 \pm 1.2) \times 10^7$
ΔG_{ad} (kJ/mol)	-44 ± 1	-43 ± 1
Γ_s (mol/cm ²)	$(2.7 \pm 0.1) \times 10^{-11}$	$(2.6 \pm 0.1) \times 10^{-11}$

layers of transition metal complexes by considering two models.^{23,24} One assumes kinetic control of the system while the other assumes fast adsorption with mass transport or diffusion control. In both cases the adsorption process is assumed to follow the Langmuir isotherm. The expression describing the variation in the surface coverage (Γ_t) with time (t) for the kinetic control model is

$$\Gamma_t = \Gamma_e (1 - e^{-kC^*t}) \quad (5)$$

where Γ_e is the equilibrium coverage, k is the adsorption rate constant, and C^* is the adsorbate bulk concentration. For the diffusion control model the equation is

$$\Gamma_t = \sum a_j (Dt)^{j/2} \quad (6)$$

where D is the diffusion coefficient of the adsorbate and a_j ($j = 0, 1, 2, \dots$) are a series of constants, dependent on D and C^* . The limiting case under these conditions is the one corresponding to zero concentration of the adsorbate in the vicinity of the surface until the corresponding equilibrium coverage is reached. Under these conditions, $a_0 = 0$ and $a_1 = 2C^*/\sqrt{\pi}$, so that the kinetics can be described as

$$\Gamma_t = 2C^* \sqrt{Dt/\pi} \quad (7)$$

Here we should bear in mind that (5) and (7) are the two limiting (and simpler) cases. We shall employ these two models to fit the experimental data and determine which one better describes the experimental observations.

Figure 3 presents the kinetic data for PLA₂ adsorption onto a mercury electrode surface at various PLA₂ solution concentrations. The symbols are experimental data while the lines are fits using the above-mentioned models. It can be seen that at the higher concentrations ($>0.1 \mu\text{M}$) the kinetic control model shows an excellent fit (Figure 3a), indicating that this model is most applicable under these conditions. However, at lower concentrations ($<0.05 \mu\text{M}$), neither (5) nor (7) shows a good fit to the experimental data (Figure 3b), suggesting that under these conditions the kinetic process is not well represented by the above-mentioned limiting cases. However, an excellent fit

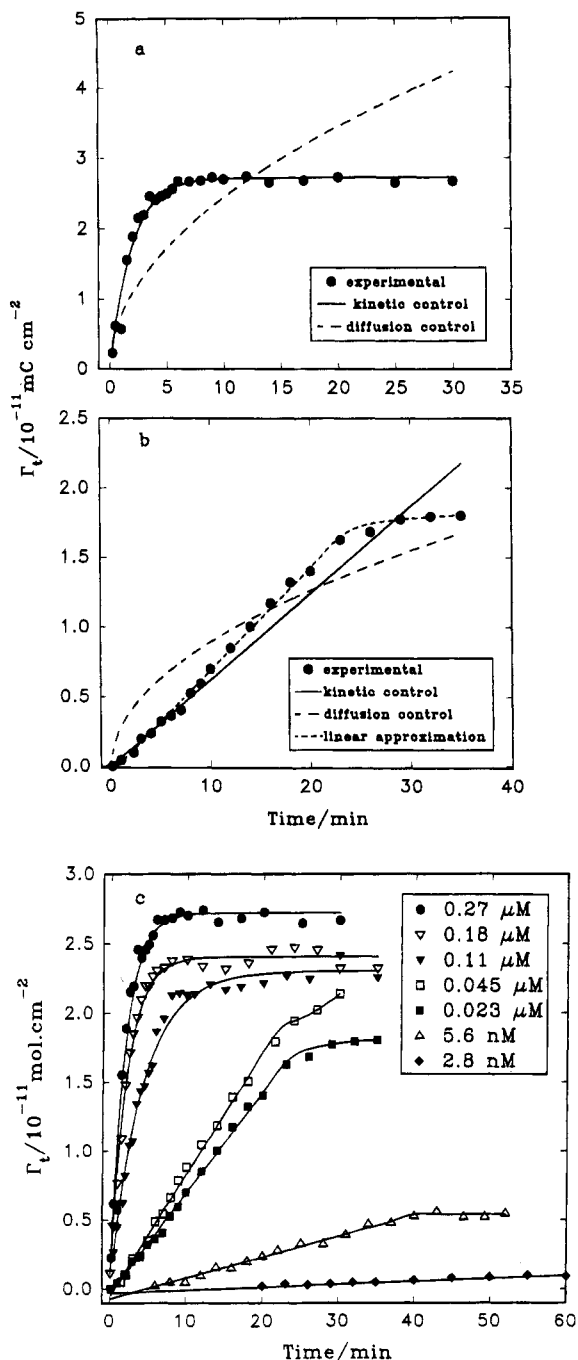


Figure 3. Adsorption kinetics of PLA₂ at various concentrations in 0.20 M KCl buffered with 0.01 M K₂HPO₄-KH₂PO₄ (pH 6.70) at room temperature (22 °C). (a) [PLA₂] = 0.27 μM. (b) [PLA₂] = 0.023 μM. (c) Kinetic data with corresponding best fits depending on the specific concentration.

was found using the expression

$$\Gamma_t = k'(t - t_0) \quad (8)$$

where k' and t_0 are the fitting parameters, for the rising part of the adsorption profiles. Figure 3c shows the fits of the kinetic data over the concentration range 2.8 nM to 0.27 μM either to the kinetically controlled model (eq 5) or by linear fitting (eq 8), depending on the specific concentration. In all cases it can be seen the fits are all quite good.

Mathematically, eq 8 can be described as the first term of the Taylor expansion of eq 5. When kC^* is small, this is a very good approximation to eq 5. Thus, this would suggest that even at concentrations of the order of nanomolar, the

TABLE 2: Induction Time (t_0) as a Function of PLA₂ Concentration^a

[PLA ₂] (μM)	t_0 (min)	[PLA ₂] (μM)	t_0 (min)
0.0450	0.7 ± 0.2	0.0056	4.8 ± 0.6
0.0225	0.6 ± 0.2	0.0028	15 ± 4
0.0113	3.1 ± 0.4		

^a Experiments were carried out in 0.20 M KCl buffered with 0.010 M K₂HPO₄-KH₂PO₄ (pH 6.7) at room temperature.

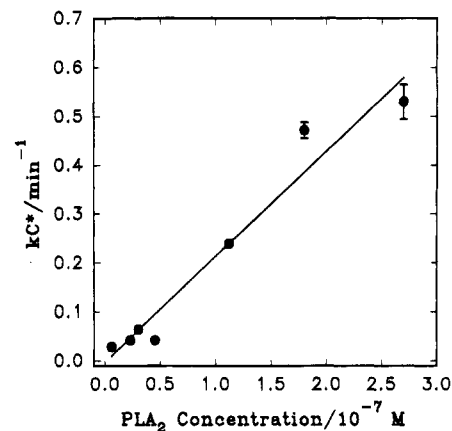


Figure 4. Variation of adsorption rates with PLA₂ concentration. Experimental conditions are identical to those in Figure 2.

adsorption dynamics still follow the kinetically controlled model. Thus, eq 8 can be recast as

$$\Gamma_t = \Gamma_e kC^*(t - t_0) \quad (9)$$

where Γ_e is the equilibrium coverage at a given bulk concentration (C^*) and can be determined from the plateau portion of the profiles. The nonzero t_0 would indicate that there is an induction time prior to the actual adsorption process. A similar situation was observed in the adsorption, from very low solution concentration, of redox-active self-assembling monolayers of Os complexes onto a Pt surface.²² Microscopically, this would suggest that a certain local concentration of the adsorbate must be reached prior to adsorption. From Table 2, one can see that t_0 increases with a decrease in PLA₂ concentration, which is consistent with the above argument.

Figure 4 shows the fitting parameter (kC^*) of the kinetics curves as a function of PLA₂ concentration (C^*), where the slope equals the rate constant (k). From Figure 4, we can estimate the rate constant (k) to be $(3.6 \pm 0.4) \times 10^4 \text{ s}^{-1}$. The linearity of this plot is again consistent with the Langmuirian kinetic behavior of this system.

From the above study, one can conclude that the adsorption process of PLA₂ onto mercury is kinetically controlled over the concentration range of 2.8 nM to 2.7 μM, with an adsorption rate constant of $(3.6 \pm 0.4) \times 10^4 \text{ s}^{-1}$. The observation of an induction time is consistent with the kinetic control mechanism.

4. pH Dependence of the Adsorption Kinetics. We also investigated the effects of electrostatic interactions on the kinetics of adsorption by varying the solution pH. Figure 5 shows adsorption kinetics plots at various pH values, with, again, the symbols being experimental data and the solid lines the fits. At low pH (pH < 2.5), an excellent fit was found to eq 5 whereas at higher pH (pH > 4.6), better fits were found using eq 8. As mentioned earlier, this indicates that over the pH range studied (0.77–8.50) Langmuir adsorption kinetics are still followed. During the adsorption process, the electrode potential was held positive of the corresponding open circuit potential, which is very close to the potential of zero charge (pzc).

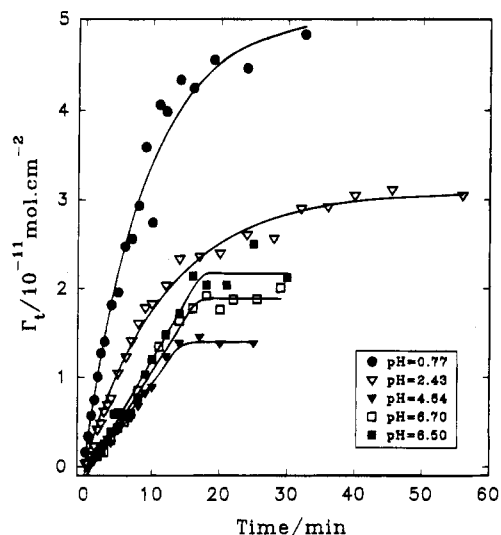


Figure 5. Adsorption kinetics at various pH values at a PLA₂ concentration of 0.030 μ M and at room temperature.

However, due to specific adsorption of chloride on the electrode surface, there is likely an overall negative interfacial charge.²⁵ As the interfacial kinetics would be anticipated to be affected by interfacial electrostatics, one would expect that the variation of the electrostatic interactions between the electrode and the PLA₂ molecules would result in variations of the adsorption processes including surface coverage and adsorption kinetics. The isoelectric point (pI) of free PLA₂ is about 7.4,¹⁴ so that at pH < 7.4, the PLA₂ molecule is positively charged whereas at pH > 7.4, it is negatively charged. In addition, the lower (higher) the pH, the more positive (negative) charges the PLA₂ molecule carries. Recalling that the interfacial electric field is negative (with amplitudes varying with electrode potential), there will be an electrostatic attraction between the electrode surface and the PLA₂ molecules at pH < 7.4 and repulsion at pH > 7.4. These electrostatic interactions will decrease as the difference between the applied potential and the pzc decreases. In our experiments, we varied the electrode potential at different pH with the values being 0.0 V at pH = 0.77 and 2.43, -0.20 V at pH = 4.64, and -0.25 V at pH = 6.70 and 8.50 (all vs Ag/AgCl), and these were chosen relative to the specific formal potential of adsorbed PLA₂ at various pH. From Table 4, it can be seen that these applied potentials are about 200 mV positive of the corresponding formal potentials for adsorbed PLA₂ at the given pH. As can be ascertained, the difference between the applied potential and the pzc decreases with increasing pH so that attractive interactions would also decrease. Thus, from the combined results of the applied electric field and the charged state of PLA₂ molecules, one would anticipate that the attractive electrostatic interactions between the interface and the PLA₂ molecule increase with a decrease in pH, and consequently the adsorption rate increases, as shown in Figure 6. Here one should bear in mind that the electrostatic interaction between the interfacial electric field and the charged PLA₂ molecules is relatively weak, due to the fact that the amplitude of the electric field is small and the overall charge density of PLA₂ molecules is rather low because of their large size. Thus, it can be seen that the previous experimental observation that over the entire pH range of 0.77–8.5 the adsorption process followed Langmuirian kinetics is consistent with the above argument, as under these specific pH conditions the interaction between the electrode interface and the PLA₂ molecules is that of a weak attraction, with a small variation in the amplitude. One exception is at pH = 8.50, where the interaction is repulsive, different from the other cases. However, as men-

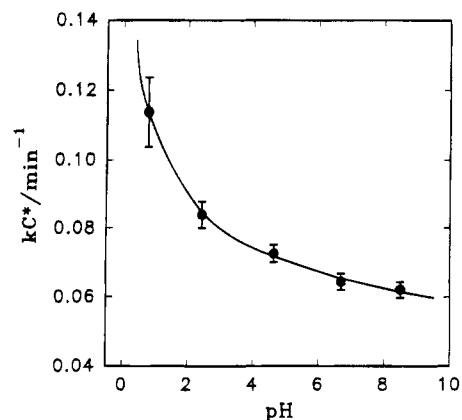


Figure 6. Variation of adsorption rate with solution pH under the same experimental conditions as in Figure 5.

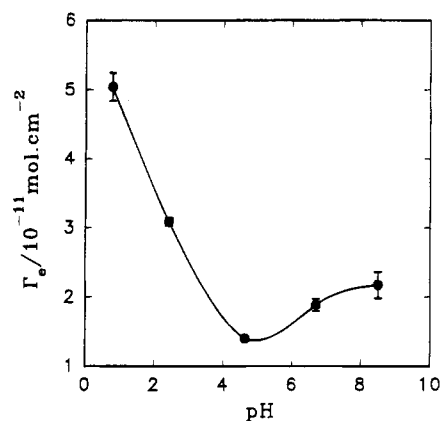


Figure 7. Equilibrium coverage of PLA₂ at various solution pH values and under the same experimental conditions as in Figure 5.

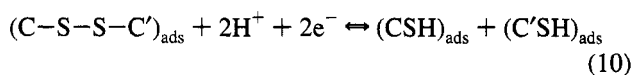
tioned above, the negative interfacial electric field is weak and the negative charge of the PLA₂ molecules is small at pH = 8.50, so that this repulsion will not be expected to hinder the adsorption kinetics dramatically. Thus, the overall kinetics still follows the same mechanism, as anticipated.

Having discussed the pH effects on the kinetic aspects of the adsorption process where interfacial interactions play a significant role, we now focus on the effects of pH on the adsorption thermodynamics. Figure 7 shows the pH dependence of the equilibrium surface coverage at a solution concentration of PLA₂ of 0.030 μ M; one can see that the coverage decreases rapidly with increasing pH, reaches a minimum at pH = 4.64, and afterward increases slowly with further increases in pH. To account for this behavior, one should note that, at very low pH values (pH < 2.5), the salt bridges within the PLA₂ molecules will likely be destroyed although the disulfide bonds are probably still maintained. Thus, the molecular conformation will be changed. It is likely that the PLA₂ molecules may have been denatured at very low pH, becoming coil-like and thus allowing closer packing of the adsorbed molecules and hence a higher equilibrium coverage. In addition, it is also likely that there is still only one disulfide group per PLA₂ molecule attached to the mercury surface. However, if the enzyme is denatured, it would also be possible to have more than one disulfide bond in contact with the electrode surface. We do not believe this to be the case since that would likely require that the enzyme be adsorbed in a more horizontal orientation relative to the electrode surface which would greatly increase the projected area per molecule and thus would result in a decrease in the equilibrium coverage, which is contrary to the observed increase. The above arguments are also consistent with the experimental observation of a smaller value of the full

width at half maximum (fwhm) for the voltammetric peaks compared to the other cases at higher pH (Table 3). For an ideal reversible electrochemical reduction/oxidation of an adsorbed species, the fwhm of the corresponding cyclic voltammetric wave should be $90.6/n$ mV (at 25 °C), assuming no interactions between the adsorbed species. For our system $n = 2$; thus ideally the fwhm should be 45.3 mV. However, the fwhm can be affected by a variety of factors, among which an important one is the intermolecular interactions of the adsorbates with repulsive interactions giving rise to broader waves, and vice versa. In Table 3, one can see that over the entire pH range the fwhm's are greater than the ideal value even when extrapolated to zero sweep rate in order to eliminate any kinetic effect, suggesting that there exist repulsive interactions between the adsorbed species, consistent with the earlier discussion. At low pH (pH < 2.5), the fwhm's would be expected to be the largest compared to the high pH cases if the molecular conformation was still preserved, since at low pH the molecules would carry the most charges which would give rise to the greatest interaction (repulsion in this case) among the adsorbed molecules. However, the experimental observation contradicts this (Table 3), which again suggests that the molecular conformation might have changed due to denaturing. On the other hand, over the pH range 4.64–8.50, the PLA₂ molecule is stable and its conformation is preserved; thus, the similarity of their corresponding fwhm's would reflect a similar level of the intermolecular interactions.

As to the equilibrium coverages at pH > 4.64, one would expect that the repulsive intermolecular interactions of the adsorbed PLA₂ molecules would play a role in determining the equilibrium coverage. Compared with the other two cases of pH = 6.70 and 8.50, at pH = 4.64 the molecules carry the most (positive) charges and experience the greatest repulsive interaction, therefore giving rise to the lowest equilibrium coverage. In the cases of pH = 6.70 and 8.50, both pH values are in the vicinity of the pI, so that one would expect only a small charge on the adsorbed molecules and thus only small electrostatic interactions among the adsorbed molecules, resulting in a higher equilibrium coverage.

Another important aspect is the formal potential for adsorbed PLA₂. As mentioned earlier, we believe that the observed electrochemical response arises from the reduction/oxidation of the cystine residues of the adsorbed phospholipase molecules, with the overall reaction expressed as



where C and C' are the two half-cystine residues. From eq 10 and applying the Nernst equation, one can obtain that

$$\phi = \phi_0 + \frac{RT}{2F} \ln \frac{[(C-S-S-C')_{\text{ads}}][H^+]^2}{[(CSH)_{\text{ads}}][(C'SH)_{\text{ads}}]} \quad (11)$$

From (11) one can write

$$\phi = \phi_0 - \frac{2.303RT}{F} \text{pH} + \frac{2.303RT}{2F} \log \frac{[(C-S-S-C')_{\text{ads}}]}{[(CSH)_{\text{ads}}][(C'SH)_{\text{ads}}]} \quad (12)$$

which predicts a linear dependency of the formal potential with pH and with a -59 mV shift per pH unit change at 25 °C. Table 4 lists the experimental values of the formal potentials of adsorbed PLA₂ under various pH conditions, and Figure 8 depicts the variation of the redox potential with solution pH. Here the symbols are experimental data which have been

TABLE 3: Full Width at Half-Maximum (fwhm, mV) of the Cathodic Peaks at Various pH

pH	fwhm (50 V/s)	fwhm ^a (0 V/s)
0.77	146	91
2.43	174	
4.64	164	156
6.70	190	147
8.50	214	156

^a Obtained by extrapolating to $v = 0$ V/s.

TABLE 4: Effect of Solution pH on the Formal Potential of Porcine Pancreatic Phospholipase A₂ (PLA₂) Adsorbed on a Mercury Electrode Surface at 25 °C

pH	E/V vs Ag/AgCl satd	pH	E/V vs Ag/AgCl satd
0.77	-0.176 ± 0.002	6.70	-0.565 ± 0.003
2.43	-0.223 ± 0.001	8.50	-0.719 ± 0.006
4.64	-0.432 ± 0.004		

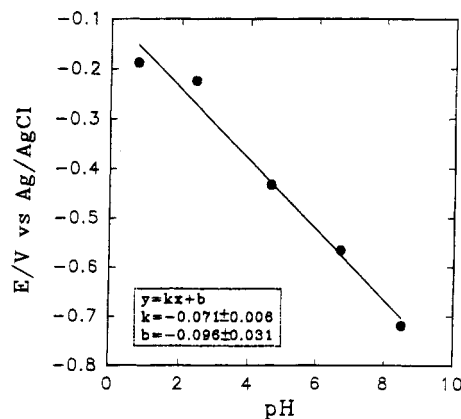


Figure 8. Dependence of the formal potential of PLA₂ on solution pH. All potentials have been corrected to be vs the reference electrode potential at 25 °C.

corrected to be referred to the same reference electrode at 25 °C by using the temperature coefficient of Ag/AgCl reference electrode, $d\phi/dT = -4.8564 \times 10^{-4}$ V/°C,²⁶ while the solid line is the fit. The linear dependency of the formal potential with pH is clearly evident. However, the plot has a slope of -71 ± 6 mV per pH unit, which is somewhat higher than the anticipated value of -59 mV mentioned above. We are, at the present, uncertain as to the specific origin of this effect, however, the fact that molecules such as PLA₂ have multiple sites that can undergo protonation could, at least in part, be responsible for this.

It appears that, during the adsorption process, the main governing force is that between the interfacial electric field of the electrode and the PLA₂ molecules. Over the entire pH range under study, the adsorption process appears to be kinetically controlled, with the adsorption rate decreasing with increasing pH, which can be interpreted as being due to the electrostatic interactions between the electrode and the PLA₂ molecules.

5. Temperature Effect on the Adsorption Kinetics. We have also carried out temperature dependence experiments. Figure 9 shows the kinetic data at various temperatures from 22.0 to 48.5 °C. The best fits were found with eq 5, indicating that the adsorption process is again kinetically controlled over this experimental temperature range.

Figure 10a shows the dependency of the adsorption rate on solution temperature. An abrupt increase is observed between 22 and 30 °C, with only a much smaller increase for temperatures of up to 50 °C. Figure 10b shows the corresponding Arrhenius plot where a break point at 31.8 °C is clearly marked. The apparent activation energy (E_a) of adsorption can be

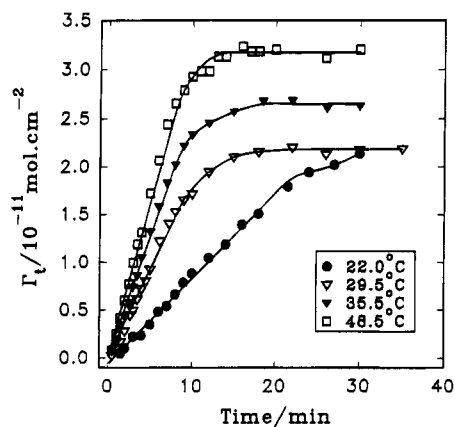


Figure 9. Adsorption kinetics of PLA₂ at various temperatures at a PLA₂ concentration of 0.045 μM and a solution pH of 6.70. Sweep rate is 50 V/s.

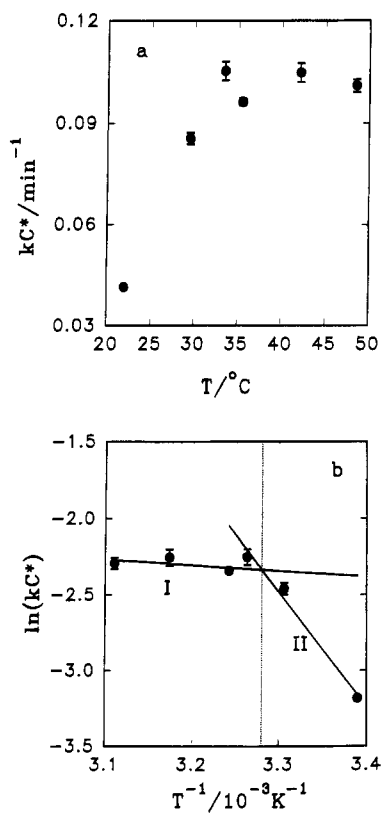


Figure 10. Dependence of adsorption rates on solution temperature with the same experimental conditions as in Figure 9: (a) adsorption rates vs temperature (°C); (b) the corresponding Arrhenius plot of (a), with dashed line marking the breaking point.

estimated for the two temperature regimes (I and II). We obtain values of 3.13 kJ/mol when the temperature is above 31.8 °C (I) and 62.3 kJ/mol when it is below (II). Such discontinuous Arrhenius plots have been previously described for some soluble enzymes when interacting with their substrates, where the discontinuity is believed to be due to a temperature-induced conformational change of the enzyme.²⁷⁻²⁹

The assertion that there are two molecular conformations depending on the solution temperature is also supported by the cyclic voltammograms for the adsorbed phospholipase at different temperatures (Figure 11). One can see that with increasing temperature, the electrochemical response of the adsorbed phospholipase molecules evolves from a single cathodic wave at room temperature to two cathodic peaks with the additional wave appearing at a more negative potential. At even higher temperatures the second cathodic wave becomes

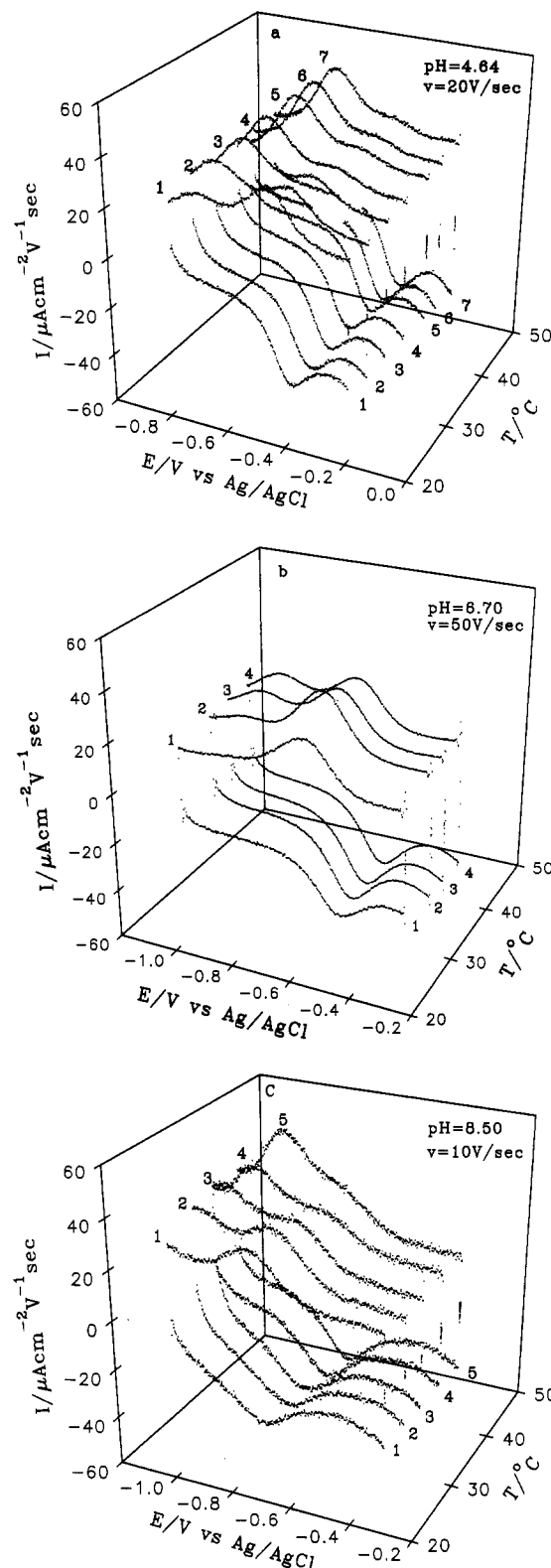


Figure 11. Cyclic voltammograms of PLA₂ at various temperatures at a PLA₂ concentration of 0.030 μM: (a) pH = 4.64, sweep rate = 20 V/s; (b) pH = 6.70, sweep rate = 50 V/s; (c) pH = 8.50, sweep rate = 10 V/s.

the main electrochemical feature, as is clearly apparent in Figure 11. It should be noted that all of the cyclic voltammograms in Figure 11 are the first cycle of scans at each temperature. In subsequent scans the second cathodic wave was not observed, and the voltammetric response was very similar to that shown in Figure 1a. In combination with the observation that there is no return anodic wave associated with the second peak, it could be suggested that although this second conformation is energeti-

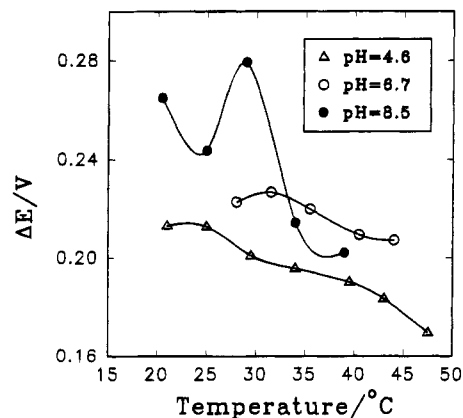


Figure 12. Variation of the difference in peak potentials (ΔE) of the two cathodic peaks with solution pH and temperature. PLA₂ concentration is 0.030 μ M in 0.20 M KCl supporting electrolyte. The ΔE values are obtained by extrapolating to zero sweep rate.

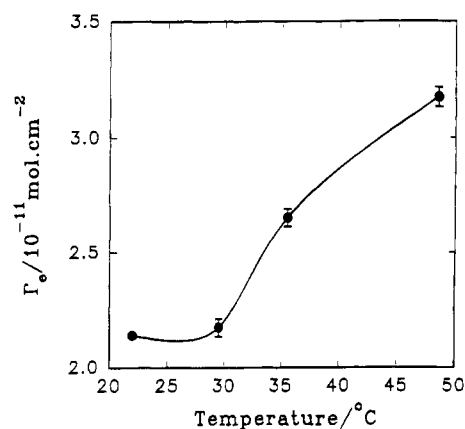


Figure 13. Variation of equilibrium coverage with solution temperature under the same experimental conditions as in Figure 9.

cally more stable, it is kinetically slow. In addition, the appearance of the second wave can only be observed at pH values above 4.6. At low pH, a single cathodic peak is always observed at all temperatures under study, which is consistent with the above-mentioned argument that under those specific pH conditions the phospholipase molecules might be denatured such that the coil-like conformation will no longer be sensitive to the solution temperature.

One interesting observation is that the potential difference (ΔE) between these two cathodic peaks appears to be a function of pH as well as temperature, as shown in Figure 12. One can see the general trend that ΔE increases with an increase in pH but decreases with increasing temperature. Since there is no return anodic wave associated with the second cathodic peak, the process likely reflects kinetics rather than thermodynamics. In addition, it could also be that a higher temperature diminishes the activation energy so that there is a smaller overpotential as depicted in Figure 12.

As to the thermodynamic aspects, Figure 13 shows the temperature effect on the equilibrium coverage at pH = 6.70, where one can see that again the entire temperature range is divided into two regimes: at temperatures below 30 °C there is little effect of temperature observed, while at higher temperatures (above 30 °C) the equilibrium coverage increases markedly with increases in temperature. This observation might be accounted for by the above argument that there exist two molecular conformations in this temperature regime. As the surface coverage from the first cycle of scans is somewhat greater than that from the subsequent continuous scans (not shown), and the subsequent scans only show a single cathodic

wave, as mentioned earlier, which corresponds to the initial conformation, it can be suggested that this conformational change gives rise to a closer packing of the adsorbed molecules and hence a higher equilibrium coverage as observed. In addition, this second conformation is likely to be more fluid since it forms at a higher temperature and would therefore give rise to a faster rate of charge propagation, again consistent with experimental observations. Moreover, these arguments are also consistent with the experimental observation that, with an increase in temperature, the second cathodic peak increases in amplitude while the other ones decrease (Figure 11).

The above discussion suggests that the molecular conformation is very sensitive to temperature with a second and different conformation appearing at higher temperature, which results in an increase in the effective surface coverage. However, as to the origin of these phenomena, further studies are required and are currently underway.

Conclusions

Cyclic voltammetry has been employed in the study of the thermodynamics of adsorption as well as the adsorption dynamics of phospholipase A₂ onto a mercury electrode surface, with emphasis on the effects of concentration, pH, and temperature.

Our findings can be summarized as follows:

(a) The cyclic voltammetric response of PLA₂ adsorbed onto a mercury surface exhibits a pair of voltammetric waves that are ascribed to cystine/cysteine residues. Although both the Langmuir and Frumkin isotherms are in qualitatively good agreement with experimental data, a better fit is obtained with the latter with an interaction parameter $g' = -0.7$, indicating the presence of repulsive, albeit small, interactions. The magnitude of the adsorption free energy is consistent with a chemisorptive bond.

(b) The adsorption process is found to be kinetically controlled over the PLA₂ concentration range of nanomolar to micromolar, based on the fits to the kinetic models.

(c) pH has a dramatic effect on the adsorption kinetics of PLA₂, most likely due to variations in the charged state of the PLA₂ molecules and consequently the variation of interactions between the electrode and adsorbed species as well as between neighboring adsorbed molecules.

(d) The conformation of the adsorbed PLA₂ molecules appears to be very sensitive to the solution temperature. A second cathodic wave was observed at higher temperatures with no corresponding return anodic wave. A temperature-dependence study showed that although this second conformation is energetically more stable, it is kinetically much slower. A discontinuity in the Arrhenius plot is ascribed to a temperature-induced conformational change of the adsorbed molecules.

A more complete understanding of the interfacial behavior of this and other phospholipases will be most valuable in further studies on their biological properties via electrochemical techniques. Further studies are underway, and results will be presented elsewhere.

Acknowledgment. This work was supported by the National Science Foundation through Grant DMR-9107116. Discussions with Dr. J. Li are gratefully acknowledged.

References and Notes

- (1) (a) Verger, R.; de Haas, G. H. *Annu. Rev. Biophys. Bioeng.* **1976**, *5*, 77–1117. (b) Verheij, H. M.; Slotbloom, A. J.; de Haas, G. H. *Rev. Physiol. Biochem. Pharmacol.* **1981**, *91*, 91–203. (c) Dennis, E. A. *Enzymes* **1983**, *16*, 308–353.
- (2) Van den Bosch, H. *Biochim. Biophys. Acta* **1980**, *604*, 191–246.

- (3) Dijkstra, B. W.; Drenth, J.; Kalk, K. H. *Nature* **1981**, *289*, 604–606.
- (4) Dijkstra, B. W.; Renetseder, R.; Kalk, K. H.; Hol, W. G. J.; Drenth, J. *J. Mol. Biol.* **1983**, *168*, 163–179.
- (5) Brunie, S.; Bolin, J.; Gewirth, D.; Sigler, P. B. *J. Biol. Chem.* **1985**, *260*, 9742–9749.
- (6) Ransac, S.; Deveer, A. M. T. J.; Rivière, C.; Slotboom, A. J.; Gancet, C.; Verger, R.; De Haas, G. H. *Biochim. Biophys. Acta* **1992**, *1123*, 92–100.
- (7) Ransac, S.; Moreau, H.; Rivière, C.; Verger, R. *Methods Enzymol.* **1991**, *197*, 49–94.
- (8) Grainger, D. W.; Reichert, A.; Ringsdorf, H.; Salesse, C. *Biochim. Biophys. Acta* **1990**, *1023*, 365–379.
- (9) Barlow, P. N.; Lister, M. D.; Sigler, P. B.; Dennis, E. A. *J. Biol. Chem.* **1988**, *263*, 12954–12958.
- (10) Menashe, M.; Romero, G.; Biltonen, R. L.; Lichtenberg, D. *J. Biol. Chem.* **1986**, *261*, 5328–5333.
- (11) (a) Jain, M. K.; Egmond, M. R.; Verheij, H. M.; Apitz-Castro, R.; Dijkman, R.; De Haas, G. H. *Biochim. Biophys. Acta* **1982**, *688*, 341–348. (b) Apitz-Castro, R.; Jain, M. K.; De Haas, G. H. *Ibid.* **1982**, *688*, 349–356.
- (12) Sundler, R.; Alberts, A. W.; Vagelos, P. R. *J. Biol. Chem.* **1978**, *253*, 5299–5304.
- (13) Colacicco, G. *Nature* **1971**, *233*, 202–204.
- (14) Scott, D. L.; Mandel, A. M.; Sigler, P. B.; Honig, B. *Biophys. J.* **1994**, *67*, 493–504.
- (15) (a) Britten, J. S.; Blank, M. *Bioelectrochem. Bioenerg.* **1977**, *4*, 209–216. (b) Nelson, A.; Benton, A. *J. Electroanal. Chem.* **1986**, *202*, 253–270. (c) Sakurai, I.; Kawamura, Y. *Biochim. Biophys. Acta* **1987**, *904*, 405–409. (d) Liu, M. D.; Leidner, C. R.; Facci, J. *J. Phys. Chem.* **1992**, *96*, 2804–2811. (e) Chen, S.; Abruña, H. D. *Langmuir* **1994**, *10*, 3343–3349.
- (16) (a) Bard, A. J.; Stankovich, M. T. *J. Electroanal. Chem.* **1977**, *75*, 487–505. (b) Heyrovsky, M.; Mader, P.; Veselá; Fedurco, M. *Ibid.* **1994**, *369*, 53–70. (c) Vavricka, S.; Heyrovsky, M. *Ibid.* **1994**, *375*, 371–373.
- (17) (a) Ralph, T. R.; Hitchman, M. L.; Millington, J. P.; Walsh, F. C. *J. Electroanal. Chem.* **1994**, *375*, 1–15. (b) Ralph, T. R.; Hitchman, M. L.; Millington, J. P.; Walsh, F. C. *Ibid.* **1994**, *375*, 17–27.
- (18) (a) De Haas, G. H.; Slotboom, A. J.; Bensen, P. P. M.; van Deenen, L. L. M.; Maroux, S.; Puigserver, A.; Desnuelle, P. *Biochim. Biophys. Acta* **1970**, *221*, 31–53. (b) Puijk, W. C.; Verheij, H. M.; De Haas, G. H. *Ibid.* **1977**, *492*, 254–259.
- (19) Trasatti, S. *J. Electroanal. Chem.* **1974**, *53*, 335–363.
- (20) Bard, A. J.; Faulkner, L. R. *Electrochemical Methods: Fundamentals and Applications*; John Wiley & Sons: New York, 1980; pp 516–518.
- (21) Waite, M. *Handbook of Lipid Research, the Phospholipase*; Plenum Press: New York, 1987; p 4.
- (22) Acevedo, D.; Bretz, R. L.; Tirado, J. D.; Abruña, H. D. *Langmuir* **1994**, *10*, 1300.
- (23) Reinmuth, W. H. *J. Phys. Chem.* **1961**, *65*, 473.
- (24) Tirado, J. D.; Acevedo, D.; Bretz, R. L.; Abruña, H. D. *Langmuir* **1994**, *10*, 1971–1979.
- (25) Grahame, D. C. *Chem. Rev.* **1947**, *41*, 441.
- (26) Bard, A. J.; Parsons, R.; Jordan, Eds. *Standard Potentials in Aqueous Solution*; Marcel Dekker: New York, 1987; p 304.
- (27) Dawes, E. A. In *Comprehensive Biochemistry*; Florin, M., Stotz, E. H., Eds.; Vol. 12, Chapter IV, pp 89–125.
- (28) Dixon, M.; Webb, E. C. *Enzymes* 2nd ed.; Longmans, Green and Company Ltd.: London, 1964; pp 145–166.
- (29) Van Tol, A. *Biochem. Biophys. Res. Commun.* **1975**, *62*, 750–756.